Research Article

Yanming Xu and Xianbin Teng*

Investigation of the lubrication performance of a marine diesel engine crankshaft using a thermo-electrohydrodynamic model

https://doi.org/10.1515/nleng-2024-0002
received December 7, 2022; accepted March 6, 2024

Abstract: This study outlines the development of a three-dimensional model for the crankshaft-bearing and a multi-body dynamics model for a four-stroke marine diesel engine. The models are constructed through a simulation approach that integrates the finite element method and multi-body dynamics method. Additionally, the Greenwood/Tripp asperity contact theory and average flow model are incorporated. The investigation also delves into the dynamic coupling between the crankshaft-bearing multi-body system and the mixed lubrication effects, accounting for lubricating oil as a thermo-electrohydrodynamic model and the journal as an elastomer. The study meticulously examines the lubrication characteristics of main bearings in marine diesel engines during normal operational conditions and scrutinizes the impact of various parameters on crankshaft-bearings. The study concludes by offering recommendations and technical support for innovative optimization design and model enhancement of diesel engine crankshaft-bearings.

Keywords: crankshaft, coupling, thermo-electrohydrodynamic theory, optimization analysis

1 Introduction

The potency of marine diesel engines is progressively escalating, accompanied by endeavors to curtail emissions and noise. The crankshaft, an intricate constituent of the diesel engine, plays a pivotal role, with its main bearing serving as a crucial friction pair directly influencing engine performance [1]. Consequently, scrutinizing the vibration and lubrication attributes of both the crankshaft and its bearing assumes substantial pragmatic and practical significance.

The authors initiate the study by constructing a three-dimensional model of the crankshaft and bearing, rooted in the structural characteristics specific to the diesel engine's crankshaft bearing. Subsequently, utilizing meshing and dynamic reduction within the finite element method [2], a multi-body dynamics model for the crankshaft bearing is developed. The lubricating characteristics of the diesel engine throughout a working cycle, under rated speed, and normal operating conditions are scrutinized, utilizing the diesel engine as the focal point of the investigation. This analysis encompasses the identification of crucial parameters such as the maximum oil film pressure and the minimum oil film thickness, serving to validate the precision of the crankshaft-bearing model. Simultaneously [3,4], the authors employ the average flow model and the Greenwood/Trip micro-convex contact theory to scrutinize influencing parameters, including crankshaft bearing clearance, lubrication system pressure, oil groove width of the lower main bearing bush, and surface roughness. These analyses aim to elucidate the characteristics of crankshaft-bearing lubrication under varying parameters. Consequently, pertinent parameters are selected to optimize the fourth main bearing of the diesel engine [5].

Expanding on prior research and considering the dynamic coupling between the crankshaft-bearing multi-body system and mixed lubrication, where lubricating oil is treated as a thermo-electrohydrodynamic (TEHD) model and the journal as an elastomer [6], this study introduces and establishes a multi-body dynamic simulation model for diesel crankshaft-bearing under diverse operational conditions and varying parameters [7]. Moreover, it scrutinizes the lubrication properties of the main bearing in standard working conditions and explores the influence of diverse parameters on the crankshaft-bearing. Additionally, the study provides valuable suggestions and technical support for innovatively optimizing the design and enhancing the model of the crankshaft and bearing.

*** Corresponding author: Xianbin Teng,** Marine Engineering Institute, Guangzhou Maritime College, Guangdong Guangzhou, 510725, China, e-mail: tengxbin@163.com, yt70231puwp69476@126.com
Yanming Xu: Marine Equipment Department, Tianjin Maritime College, Tianjin, Jinnan, 300350, China

2 Mathematical model of main bearing

The authors constructed a robust model of a four-cylinder, four-stroke diesel engine crankshaft, integrating the Greenwood/Tripp asperity contact theory [8], multi-body dynamics theory [9], average flow model [10], thermoelastic hydrodynamic lubrication theory, and finite element theory. The model comprehensively accounts for diverse influencing factors, encompassing the roughness of the crankshaft main bearing journal and shell surfaces, along with the effects of deformation and thermal considerations on the crankshaft and bearing housing.

2.1 Extended Reynolds equation based on average flow model

During the operation of a four strokes diesel engine, for the main bearing lubrication, the crankshaft journal rotates, while the upper and lower bearing shells are constrained and fixed. Therefore, the oil filling rate γ is introduced [11]. Based on the model of average flow, the dynamic load generalized Reynolds equation of the sliding bearing is established, which is solved by the finite difference method.

$$\frac{\partial}{\partial y}\left(\frac{1}{12\eta}\gamma h^3 \cdot \frac{\partial p}{\partial y}\right) + \frac{\partial}{\partial x}\left(\frac{1}{12\eta}\gamma h^3 \cdot \frac{\partial p}{\partial x}\right) = \gamma\frac{\upsilon}{2} \cdot \frac{\partial h}{\partial y} + h\frac{\upsilon}{2} \cdot \frac{\partial \gamma}{\partial y} + \frac{\partial(\gamma h)}{\partial t}. \tag{1}$$

where x and y are the equation coordinate systems [12]; t indicates the coordinate of time; p indicates the pressure of oil film; h indicates the thickness of oil film [13,14]; υ indicates the journal linear velocity; γ indicates filling rate of oil; and η indicates the lubricating oil dynamic viscosity.

The boundary conditions are set as follows:

1) Axial boundary condition

$$P = P_a\left(x = \pm\frac{B}{2}\right), \tag{2}$$

where P_a is the environmental pressure; B indicates the bearing width; and p indicates the oil film pressure.

2) Circumferential boundary conditions

At the oil film starting boundary, immediately $\gamma = 0$:

$$\begin{aligned} &P = P_{in} && |X| \le \frac{l}{2} \\ &P = P_{in}\frac{B - 2|X|}{B - l} && \frac{l}{2} < |X| \le \frac{B}{2}, \end{aligned} \tag{3}$$

where P_{in} indicates the supply pressure of oil; and l indicates the oil sump width.

$$\begin{aligned} &\frac{\partial P}{\partial \gamma} = 0 \\ &P = P_a \\ &\upsilon = \frac{y}{r}, \end{aligned} \tag{4}$$

where r is the radial coordinate.

3) Fuel supply area

$$P = P_{in}. \tag{5}$$

4) Cavity boundary condition

$$\begin{aligned} &P = P_c \quad \gamma = 1 \\ &P < P_c \quad \gamma < 1, \end{aligned} \tag{6}$$

where P_c is cavitation pressure.

2.2 Asperity contact model

By use of the Greenwood/Tripp micro convex contact theory [15], the contact pressure equation of micro convex body on the bearing surface is

$$P_b(h) = KE^*F\left(4 - \frac{h}{\sigma_s}\right), \tag{7}$$

where P_b indicates the contact pressure; K indicates the elastic contact factor; σ_s indicates the surface roughness; F is the factor of surface roughness; and E^* indicates the comprehensive elastic modulus.

If $\left(4 - \frac{h}{\sigma_s}\right) \ge 0$, we can judge a rough contact area, and in a mixed friction state; if $\left(4 - \frac{h}{\sigma_s}\right) < 0$, we can judge a fully lubricated contact area, and in a hydrodynamic lubrication state.

2.3 Oil film thickness equation

Under light load conditions, the deformation of the shells minimally affects the thickness of the oil film. However, in situations of heavy load, the impact of bearing shell and surface deformation on the oil film thickness becomes significant due to the oil film pressure [16]. This study addresses diesel engine performance across diverse conditions and loads, emphasizing the necessity to account for the elastic deformation and surface roughness of the bearing seat, shell back, and anti-friction alloy layer. In solving the generalized Reynolds equation, the roughness of the main bearing journal and shell surface is considered in each iteration step, and the oil film pressure is determined through the finite element method.

$$h(\theta) = h_{\min}(\theta) + \Delta h(\theta) + \delta h(\theta) + \sigma h(\theta). \tag{8}$$

2.4 Energy equation

In the general solution, it is assumed that the engine oil viscosity is a constant value under isothermal conditions, but in the process of accurate calculation and actual operation of the diesel engine, thermal effects and other influencing factors must be taken into account, and cavitation effects must also be considered [17]. The main bearing is subjected to alternating loads, and the transient energy equation of its work is shown in Eq. (9), which is solved discretely through the finite element.

$$\begin{aligned} &C_{\mathrm{p}}\rho\left(\frac{\partial T}{\partial t} + u\frac{\partial T}{\partial x} + v\frac{\partial T}{\partial y} + w\frac{\partial T}{\partial z}\right) \\ &= K\frac{\partial^2 T}{\partial y^2} + \eta\left[\left(\frac{\partial u}{\partial y}\right)^2 + \left(\frac{\partial w}{\partial y}\right)^2\right], \end{aligned} \tag{9}$$

where T is the fluid temperature; C_{p} indicates the fluid specific heat capacity at constant pressure; ρ indicates the density of fluid; K indicates the thermal conductivity of the fluid, x, y, and z are three coordinate axis directions, u, v, and w, respectively, denote the velocity of the fluid in the three coordinate axis directions.

Boundary conditions:

1)

$$T|_{\theta=0} = T|_{\theta=2\pi} = T_{\mathrm{mix}}, \tag{10}$$

where T_{mix} is the mixing temperature in the oil tank.

2)

$$\frac{\partial T}{\partial r}\Big|_{x=0} = 0. \tag{11}$$

3) The heat flux at the interface between oil and bearing bush is continuous:

$$\frac{\partial T}{\partial r}\Bigg|_{r=R_{\mathrm{b}}} = -K(\theta)\frac{R_{\mathrm{b}}}{C_{\mathrm{b}}K_{\mathrm{b}}h}\frac{\partial T}{\partial y}\Bigg|_{y}, \tag{12}$$

where θ is the oil film equivalent heat transfer coefficient; C_{b} is the specific heat capacity of bearing bush; K_{b} indicates the bearing pad thermal conductivity coefficient; h indicates the bearing pad convection heat transfer coefficient; and R_{b} is the outer diameter of the bearing shell.

4) The journal is regarded as an isothermal body. At the interface between oil and journal

$$T = Ts, \tag{13}$$

where Ts is the journal temperature.

2.5 Heat conduction equation of bearing bush

The diesel engine main bearing in this study is simplified [18]. The solid density is uniform, isotropic, and there is no heat source in the system. The simplified heat conduction equation is

$$\frac{\partial T}{\partial t} = \frac{K_{\mathrm{b}}}{C_{\mathrm{b}}P_{\mathrm{b}}}\left(\frac{\partial^2 T}{\partial r^2} + \frac{1}{r}\cdot\frac{\partial T}{\partial r} + \frac{1}{r^2}\cdot\frac{\partial^2 T}{\partial \theta^2} + \frac{\partial^2 T}{\partial x^2}\right). \tag{14}$$

The boundary conditions are as follows:

1)

$$T|_{\theta=0} = T|_{\theta=2\pi}. \tag{15}$$

2)

$$\frac{\partial T}{\partial x}\Bigg|_{x=0} = 0. \tag{16}$$

3) Bearing bush and oil interface

$$\frac{\partial T}{\partial r}\Bigg|_{r=R} = -K(\theta)\frac{R}{C_{\mathrm{b}}K_{\mathrm{b}}h}\frac{\partial T}{\partial y}\Bigg|_{y}. \tag{17}$$

4) Interface between bearing pad and environment

$$\frac{\partial T}{\partial r}\Bigg|_{r=R_{\mathrm{b}}} = -\frac{h_{\mathrm{b}}R_{\mathrm{b}}}{K_{\mathrm{b}}}(T|_{r=R_{\mathrm{b}}} - T_{\mathrm{a}}). \tag{18}$$

5) On both ends of the bearing

$$\frac{\partial T}{\partial x}\Bigg|_{x=\pm\frac{B}{2}} = -\frac{h_{\mathrm{b}}R_{\mathrm{b}}}{K_{\mathrm{b}}}\left(T|_{x=\pm\frac{B}{2}} - T_{\mathrm{a}}\right), \tag{19}$$

where T_{a} is the ambient temperature.

2.6 Main bearing load balance equation

The force on the journal is decomposed along Y and Z directions, excluding the inertia force of the oil film, the motion of the journal center satisfies Newton's second law of motion, the equation is as follows:

$$\begin{cases} F_y + F_{\mathrm{p}y} = m_{\mathrm{j}}R\omega_y \\ F_z + F_{\mathrm{p}z} = m_{\mathrm{j}}R\omega_z \end{cases}, \tag{20}$$

where R is the journal radius, ω_y, ω_z are the angular accelerations in y and z directions, m_{j} is the journal mass, F_y, F_z are the load components in y and z directions, $F_{\mathrm{p}y}$, $F_{\mathrm{p}z}$ are the oil film reaction force in y and z directions, respectively.

2.7 Solution scheme of expanded TEHD model

Simultaneous solution of the equation set for extended TEHD model is obtained numerically by using own computer program (Figure 1).

3 Diesel engine modeling and lubrication analysis

3.1 Diesel engine crankshaft-main bearing modeling

This study centers on the crankshaft and main bearing of a marine in-line four-cylinder stroke diesel engine. Initially, a three-dimensional finite element model encompassing the crankshaft, bearing shell, and bearing seat is established. The characteristics of the five main bearings are determined using AVL-Excite software by applying the mathematical equations, yielding essential lubrication parameters [19]. The analysis involves the identification of key lubrication characteristics, such as the maximum oil film pressure and minimum oil film thickness, throughout each load cycle for the five main bearings, providing insights into the main bearing lubrication. Figure 2 illustrates the coupling model of the crankshaft-main bearing multi-body dynamics.

In establishing the shafting parameters, essential details such as the diesel engine's operational speed, cylinder count, cylinder bore, stroke, firing sequence, geometric characteristics of the shafting, component quality, gas pressure, and other pertinent factors must be specified. The primary design performance indicators and technical parameters are succinctly presented in Table 1.

Figure 3 illustrates the temporal variation of the cylinder pressure curve at a diesel engine speed of 2,000 rpm, showcasing the fluctuation of cylinder pressure with respect to the crankshaft angle. This curve depicts the cylinder pressure obtained through fitting experimental data provided by the factory.

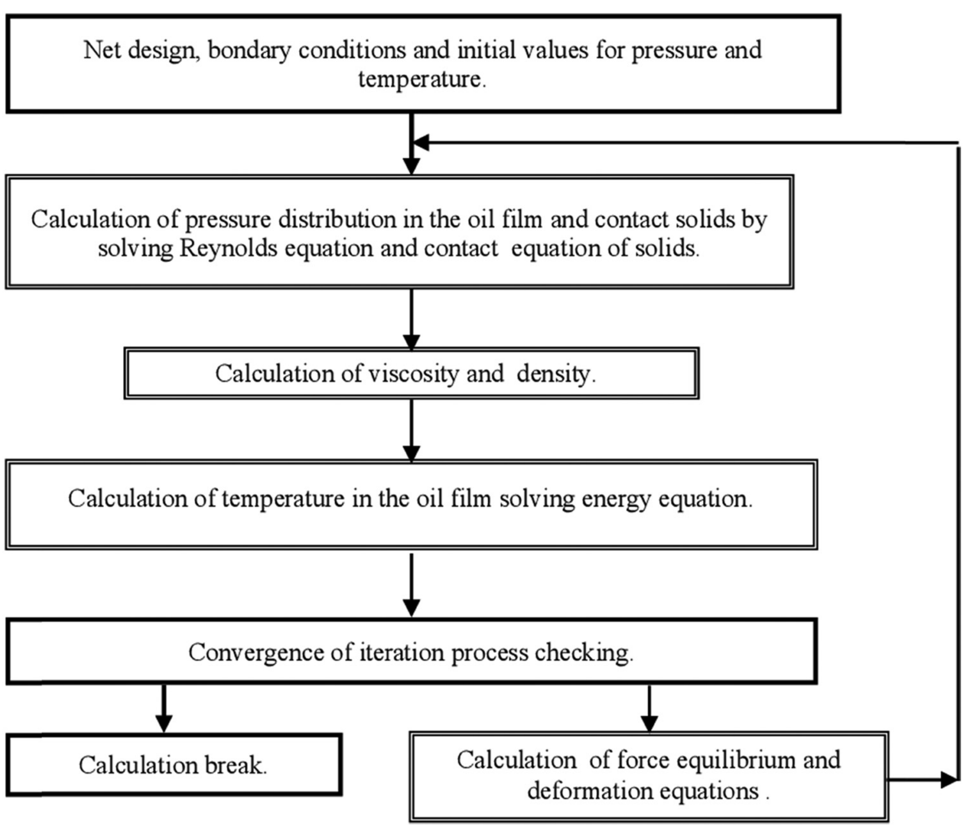

Figure 1: Solution scheme of expanded TEHD model.

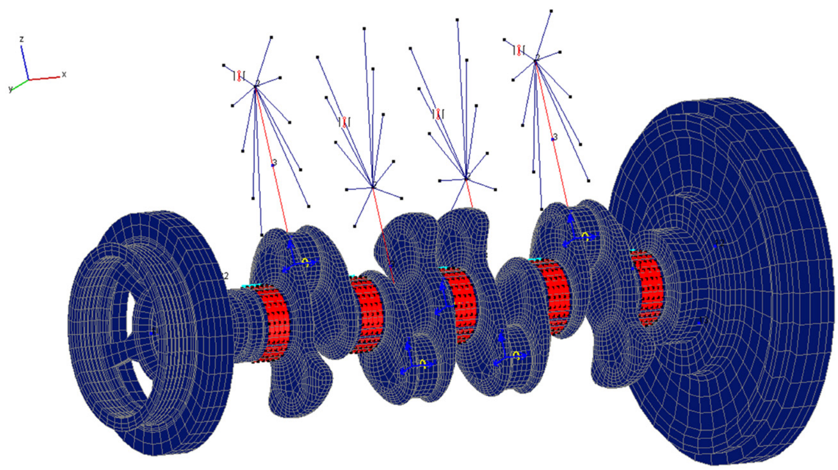

Figure 2: Multi body dynamic coupling model of diesel engine crankshaft main bearing.

Table 1: Main design performance indexes and technical parameters of diesel engine

Bearing shell width	19 mm
Bearing shell oil groove/width	270°–90°/4 mm
Oil supply pressure/temperature	0.5 MPa/90°
Main bearing journal/bearing shell nominal diameter	60 mm
Bearing clearance	25 μm
Bearing shell/journal surface roughness	0.8 μm/0.4 μm
Rated speed	2,000 rpm

3.2 Main bearing dynamic characteristics

The crankshaft main journal exhibits periodic movement due to external loads, primarily originating from gas pressure and reciprocating inertia force. As a result, the vibration pattern of the crankshaft relies mainly on the forcing actions exerted by cylinder pressure and reciprocating inertia force.

Figure 4 presents the calculated oil film reactions for each main bearing. The peak oil film reaction values for the five main bearings are 33,720, 45,293, 32,097, 43,041, and 35,985 N, respectively. Among them, the peak values for No. 2 and No. 4 main bearings are the highest, followed by No. 1 and No. 5 bearings. The oil film force peak value of No. 3 main bearing, located in the middle, is the smallest, primarily determined by the relative positions of the firing cylinder and the main bearing. When a cylinder fires, the oil film reaction of adjacent main bearings undergoes a significant change, with impacts propagating from near to far. At a crank angle of 180°, when No. 2 cylinder fires, main bearings No. 2 and No. 3 are most affected, resulting in the maximum oil film reaction for these bearings. The oil film reaction of No. 1 and No. 4 main bearings also fluctuates. The influence on No. 5 main bearing is the least,

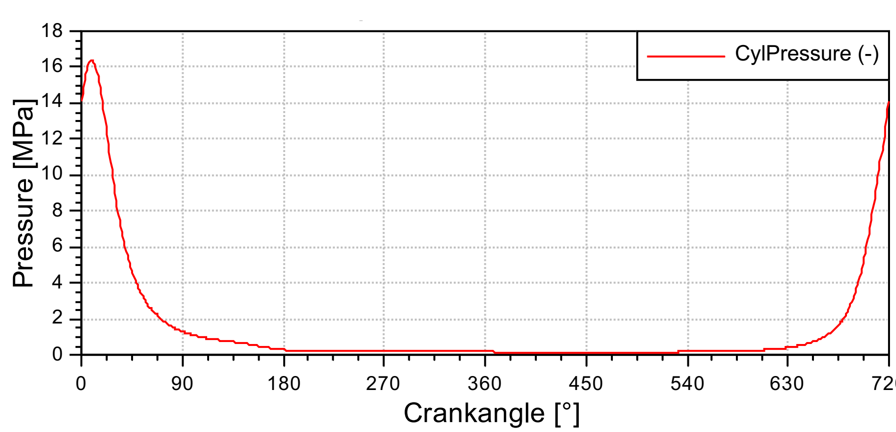

Figure 3: Cylinder pressure curve of diesel engine.

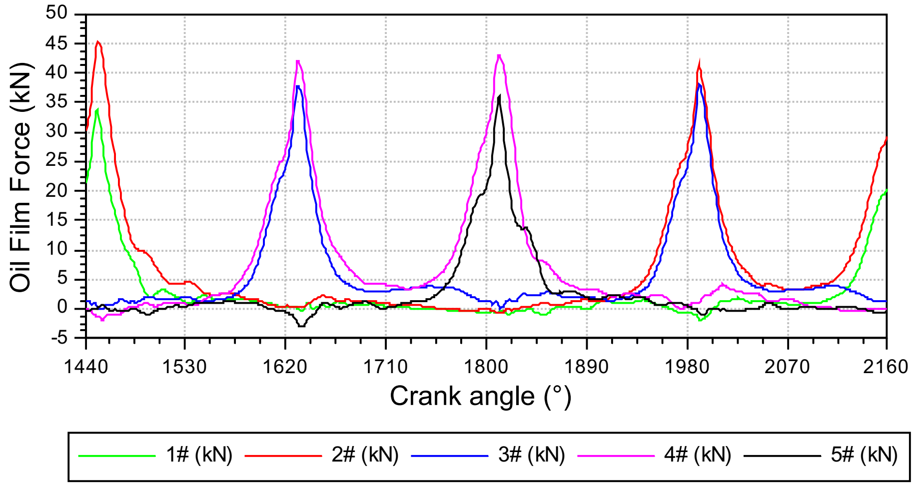

Figure 4: The oil film reaction of main bearing.

given its greater distance from the firing cylinder. Additionally, the oil film reaction forces of main bearings 2 and 3 differ due to the inertia forces of adjacent cylinders.

3.3 Main bearing lubrication analysis

The lubrication condition of the diesel engine directly affects its operational performance, making continuous research on the lubrication system essential. The optimal lubrication state for the main bearing is hydrodynamic lubrication [20]. The wedge-shaped structure created by the crankshaft and bearing forms a hydrodynamic oil film, which sustains the external load and prevents direct contact between the crankshaft and bearing, effectively reducing friction and wear.

Figure 5 presents a comparison of the maximum oil film pressure in the five main bearings during normal operation. The figure reveals distinct oil film pressure variations for the four working processes of the diesel engine on the crankshaft-bearing. As the engine approaches the third working stroke, the oil film pressure increases, and vice versa. For example, in the case of the 3# main bearing, the maximum crank angle for the oil film pressure occurs at 1,620° CA and 1,980° CA, precisely when the second and third cylinders are performing work, with almost no impact on the oil film pressure in other main bearings.

The comparison of the minimum oil film thickness in the five bearings under normal operation is illustrated in Figure 6. The minimum thickness of the oil film for the first, second, third, fourth, and fifth main bearings are 1.04, 1.23, 1.18, 1.23, and 1 μm, respectively.

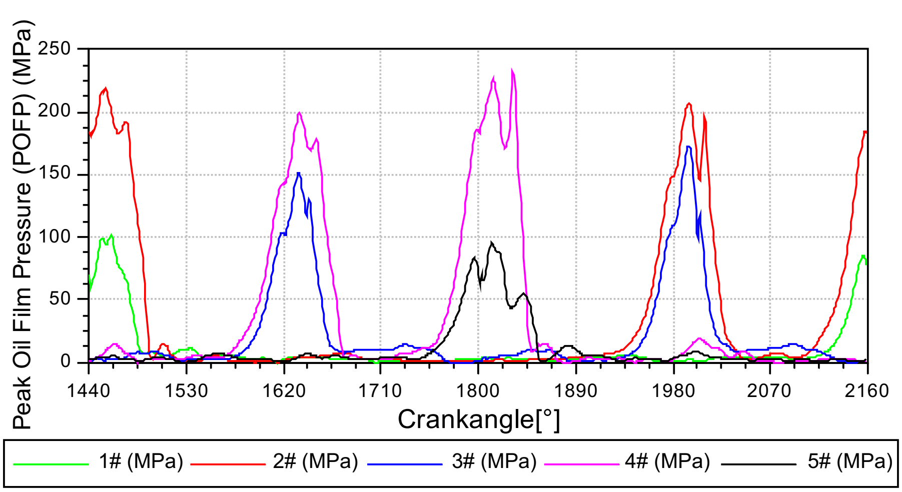

Figure 5: Comparison diagram of five main bearings maximum oil film pressure.

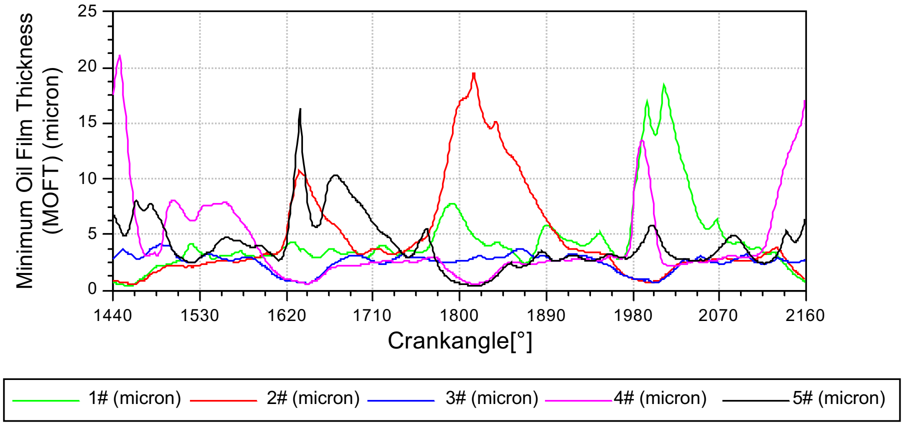

Figure 6: Comparison of five main bearings minimum oil film thickness.

The minimum oil film thickness represents the smallest value formed by the diesel engine main bearing during operation. According to the formation mechanism of hydrodynamic lubrication, the minimum thickness of the oil film should be at least five times the surface roughness of the main bearing and main journal. A comparison of the recommended minimum oil film thickness by various internal combustion engine research institutes indicates that the Austrian Liszt Institute requires a minimum main bearing oil film thickness of 1.2–1.4 μm. However, the oil film thicknesses of the 1#, 3#, and 5# main bearings are all lower than this value, suggesting the possibility of contact between the bearing shell and the journal, leading to mixed friction.

4 Influence of changing parameters on crankshaft bearing lubrication

During the operation of the diesel engine, the lubrication remains in a normal state. Based on the above simulation results, we selected the fourth bearing as the research subject to investigate its influence on the crankshaft lubrication characteristics by varying the crankshaft bearing clearance, lubrication system supply pressure, width of the main bearing lower oil groove, and the journal surface roughness. Concurrently, we identify the optimal parameters for achieving liquid dynamic lubrication during diesel engine operation through comparative analysis.

4.1 Oil groove width

Theoretical studies by Reynolds on lubrication characteristics indicate that the variation in oil groove width significantly impacts lubrication characteristics. Based on the original oil groove width of 19 mm, dynamic simulations were conducted using three other oil groove widths: 17.6, 18.2, and 19.8 mm.

Figures 7 and 8 illustrate that with an increase in the oil groove width, the minimum thickness of the oil film also increases, while the maximum oil film pressure initially decreases and then increases. The main reason for this behavior lies in the impact of reduced oil groove width on the lubricating oil flow over the bearing shell surface,

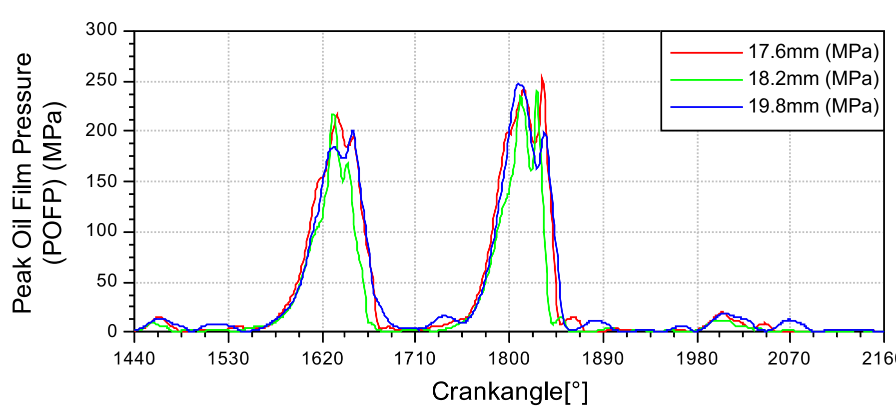

Figure 7: Comparison diagram of 4 # main bearing maximum oil film pressure under different bearing widths.

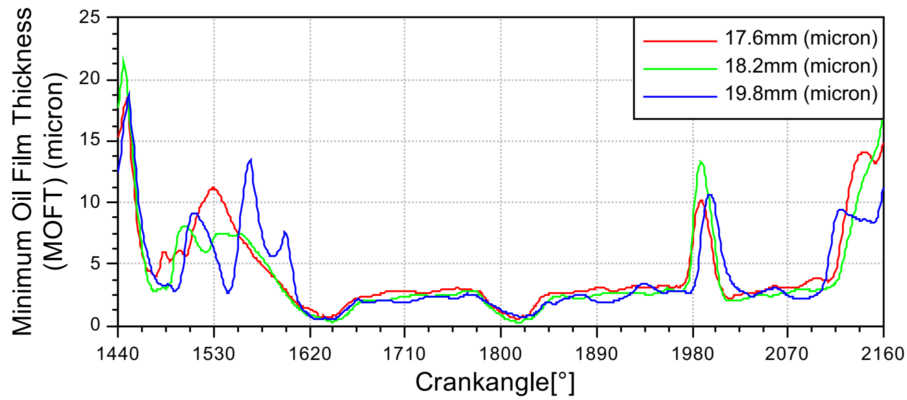

Figure 8: Comparison diagram of 4 # main bearing minimum oil film thickness under different bearing widths.

leading to an elevated load per unit area in the upper and lower directions of the bearing shell. Consequently, during engine operation, the oil flow becomes less smooth, causing a reduction in the minimum oil film thickness. Conversely, an increased oil groove width reduces the load per unit area in the upper and lower directions of the bearing shell, leading to improved lubrication. Sufficient lubricating oil can then lubricate the bearing shell and journal surface, strengthening the oil film lubrication oscillation effect and increasing the minimum oil film thickness. Simultaneously, the peak contact pressure decreases. Nevertheless, considering the overall factors, an appropriate bearing width is crucial for ensuring hydrodynamic lubrication. The ideal groove width should neither be too large nor too small, but rather optimized to achieve the best lubricating oil flow and oil film thickness.

4.2 Oil supply pressure

Figures 9 and 10 illustrate the variation in oil supply pressure from 0.3 to 0.6 MPa, while keeping parameters such as oil groove width, journal surface roughness, and bearing clearance unchanged. The maximum pressure of the oil film, minimum oil film thickness, average frictional power consumption, and peak contact pressure between the crankshaft and bearing show little change under these conditions. However, with an increase in oil supply pressure, the lubricating oil flow also increases, which has little effect on the lubrication properties of the crankshaft and bearing. Generally, the normal oil supply pressure for diesel engines can be adequately met. Any pressure drops should be promptly investigated to prevent adverse reactions due to bearing oil shortage.

4.3 Bearing clearance

Figures 11 and 12 show that an increase in the bearing clearance leads to a decrease in the minimum oil film thickness and an increase in the maximum pressure of the oil film. Excessively large clearance results in increased oil leakage from the bearing surface, leading to larger flow

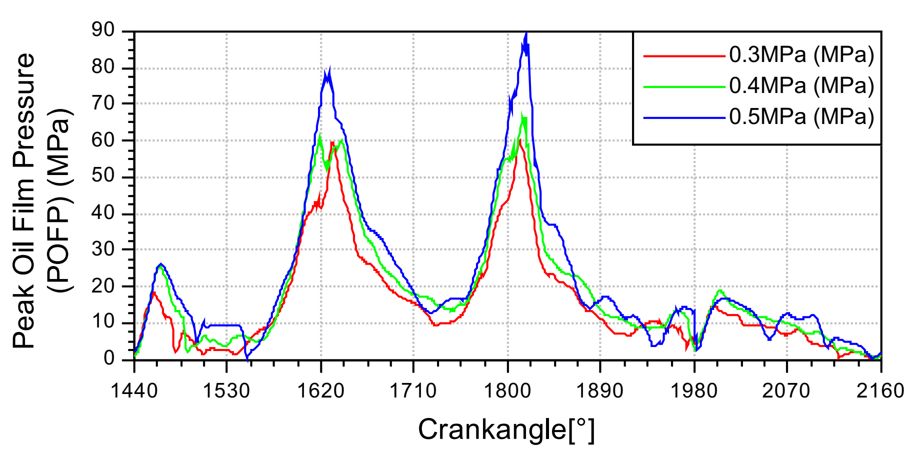

Figure 9: Comparison diagram of 4 # main bearing maximum oil film pressure under different oil supply pressures.

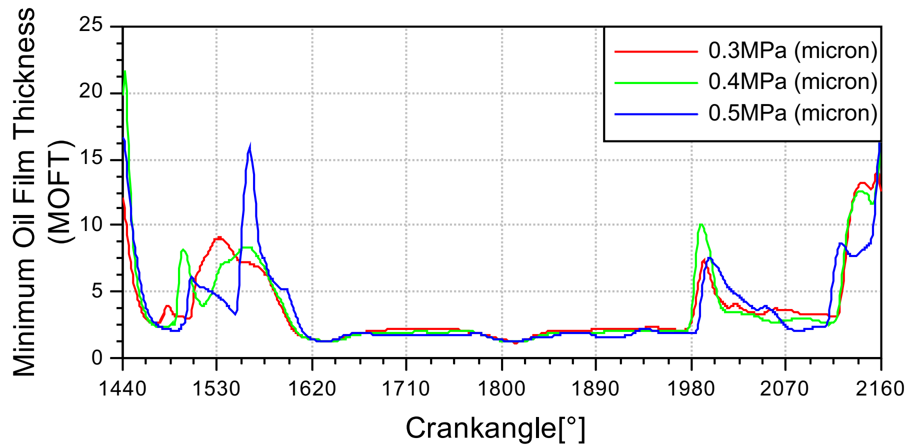

Figure 10: Comparison diagram of 4 # main bearing minimum oil film thickness under different oil supply pressures.

and decreased oil film thickness. This, in turn, enlarges the contact area between the journal and bearing, deteriorating the lubrication conditions and making the bearing susceptible to damage, resulting in increased temperature and excessive vibration. Conversely, if the bearing clearance is too small, friction consumption increases, leading to insufficient oil flow and reduced oil film bearing capacity, which also hinders the achievement of effective lubrication. Based on the above analysis, the following conclusions can be drawn:

(1) An increase in bearing clearance leads to higher maximum pressure of the oil film and reduced minimum oil film thickness.
(2) Excessively small bearing clearance leads to elevated oil temperature and compromised oil film bearing capacity, making it difficult to achieve liquid dynamic lubrication. On the other hand, excessively large bearing clearance can lead to increased lubricating oil leakage and higher loads, hindering effective lubrication.

4.4 Surface roughness

Figures 13 and 14 demonstrate that an increase in journal surface roughness leads to an increase in the minimum oil film thickness and a decrease in the maximum oil film pressure, which is beneficial for lubrication. However, based on the calculation of the micro contact model, the value of $\left(4 - \frac{h}{\sigma_s}\right)$ in the model is greater than zero, indicating that the main bearing experiences mixed friction. Consequently, a large journal surface roughness promotes the formation of an oil film, but the lubrication state is still not optimal.

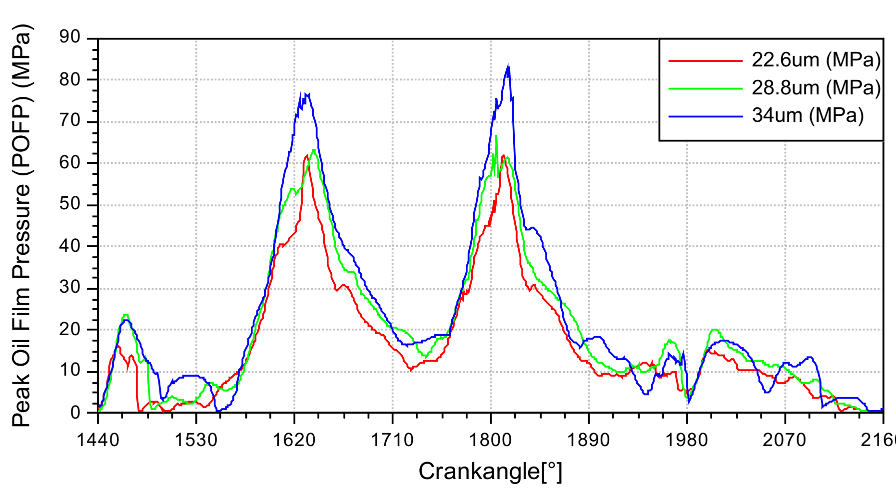

Figure 11: Comparison diagram of 4 # main bearing maximum oil film pressure under different bearings clearances.

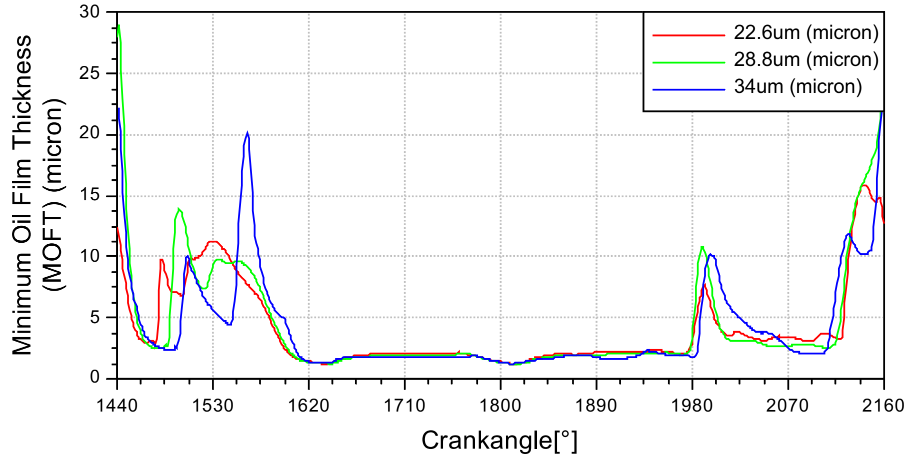

Figure 12: Comparison diagram of 4 # main bearing minimum oil film thickness under different bearing clearances.

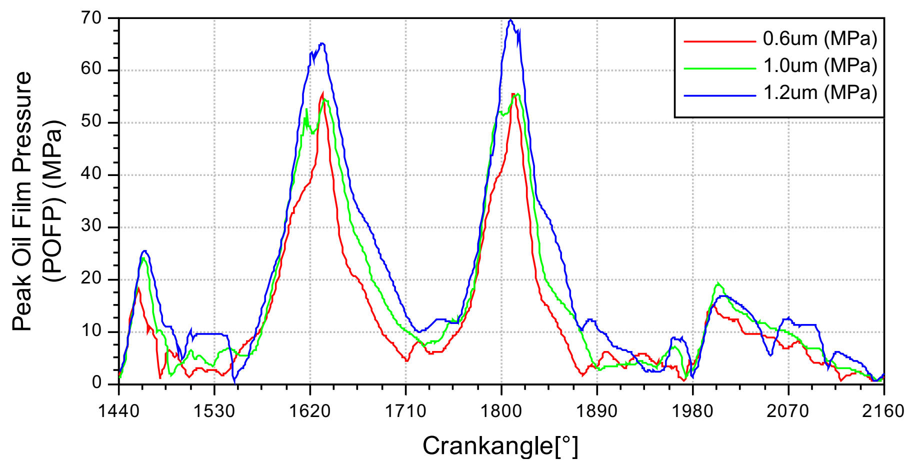

Figure 13: Comparison diagram of 4 # main bearing maximum oil film pressure under different roughness.

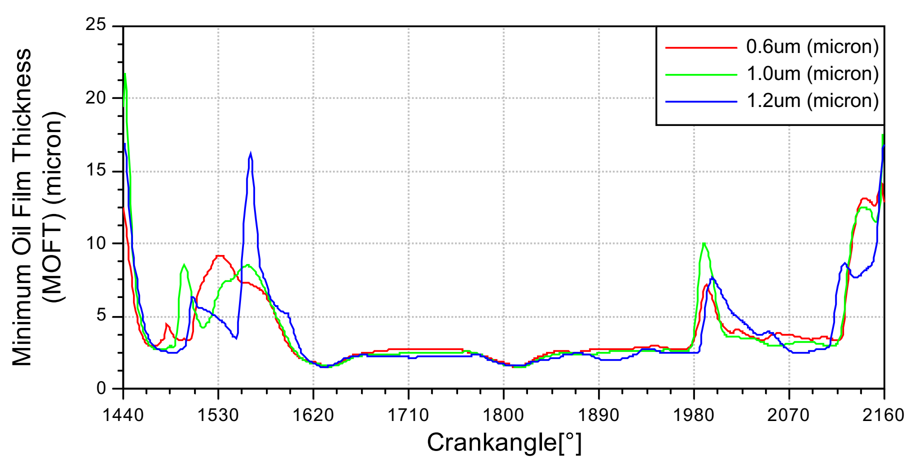

Figure 14: Comparison diagram of 4 # main bearing minimum oil film thickness under different roughness.

Table 2: Optimization scheme

	Oil groove width (mm)	Lubricating oil pressure (MPa)	Bearing clearance (mm)	Roughness (μm)
Original	19.0	0.5	25	0.8
Optimized	19.8	0.4	28.8	1

Table 3: Calculation results of the optimization

	Max. oil film pressure (MPa)	Min. oil film thickness (μm)	Average total friction consumption (KW)	Peak contact pressure (MPa)
Original	66.51	1.23	0.42	176.5
Optimized	57.8	1.36	0.37	166.8

5 Optimization design

Based on the preceding analysis of the oil groove width, lubricating oil pressure, bearing clearance, and roughness of the journal surface and their effects on the lubrication of the crankshaft-bearing model, a parameter optimization scheme for this diesel engine type is proposed in Table 2. The objective is to maintain the diesel engine in the optimal lubrication state during operation, which requires maximizing the minimum oil film thickness while minimizing the maximum pressure of the oil film.

Table 3 presents the calculation results after optimization, indicating that the maximum oil film pressure is reduced to 57.8 MPa, and the minimum oil film thickness is increased to 1.36 μm. Compared to the original scheme for the fourth main bearing, the maximum oil film pressure decreases, and the minimum oil film thickness increases, resulting in an optimized lubrication characteristic for the diesel engine's fourth main bearing.

In the optimization scheme, the objective is to maintain the maximum oil film pressure within an acceptable range to prevent the detachment of the wear-resistant alloy layer on the bearing shell's working surface. Additionally, the oil film pressure follows a parabolic distribution. With an increase in the oil groove width, there is a corresponding increase in the minimum oil film thickness. Notably, the maximum oil film pressure exhibits an initial decrease followed by an increase. This phenomenon is primarily attributed to the impact of reducing the oil groove width on lubricating oil flow over the bearing bush surface, resulting in an elevated load per unit area in the upper and lower bearing bush directions. Consequently, during diesel engine operation, the oil flow becomes less smooth, leading to a reduction in the minimum oil film thickness. Conversely, widening the oil groove diminishes the load per unit area in the bearing shell direction, improving lubrication. This enhancement allows sufficient lubricating oil to reach and lubricate the bearing shell and journal surfaces, strengthening the oscillation effect of oil film lubrication. Consequently, the minimum oil film thickness increases, and the peak contact pressure decreases. However, maintaining an appropriate bearing width is crucial to ensure hydrodynamic lubrication. Therefore, the optimal groove width should strike a balance, avoiding extremes to ensure the best lubricating oil flow and oil film thickness.

6 Conclusion

This study proposes an innovative approach for diesel engine crankshaft-bearing design, integrating finite element and multi-body dynamics for lubrication property analysis. Key findings are as follows:

1. In normal operation, the five main bearings achieve hydrodynamic lubrication within a specific crank angle, meeting the minimum oil film thickness criteria (1.2–1.4 μm) set by the Liszt Institute for Internal Combustion Engine [21–23]. Despite a misalignment with maximum bearing load, adherence to design specifications is ensured. The lack of a linear relationship between minimum oil film thickness and maximum oil film pressure suggests multiple factors determine the final oil film thickness.
2. Increasing oil groove width raises minimum oil film thickness, with an initial decrease followed by an increase in maximum oil film pressure [24–26]. Optimizing groove width is crucial for balancing effective oil flow and film thickness for hydrodynamic lubrication.

3. A larger bearing clearance increases maximum oil film pressure and reduces minimum oil film thickness [27]. Selecting an optimal bearing clearance, considering oil flow rate and working temperature, is crucial for mitigating issues associated with inadequate and excessive clearance.

Funding information: This work has not received any external funding.

Author contributions: Yanming Xu conducted experimental comparisons. Xianbin Teng conducted data collection and analysis.

Conflict of interest: The authors declare that there is no conflict of interest.

Data availability statement: Data sharing is not applicable to this article as no datasets were generated or analysed during the current study.

References

[1] Wu L, Li M, Yang X, Li L, Liang G, Qiao X. Effect of coupling weight of marine diesel engine on crankshaft vibration and lubrication. J Phys Conf Ser. 2020;1633(1):1–10.

[2] Dąbrowski K, Żurawski M, Rodak D. Model proposition of the crankshaft with tortional-bending coupling vibrations. Przegląd Mechaniczny. 2018;1(1):41–4.

[3] Gomes J, Gaivota N, Martins RF, Silva PP. Failure analysis of crankshafts used in maritime V12 diesel engines. Eng Fail Anal. 2018;92:466–79.

[4] Fonte M, Duarte P, Anes V, Freitas M. On the assessment of fatigue life of marine diesel engine crankshafts. Eng Fail Anal. 2015;56:51–7.

[5] Li W, et al. Tribological effect of piston ring pack on the crankshaft torsional vibration of diesel engine. J Technol Sci. 2015;16(7):908–21.

[6] Hoang AT. A review on fuels used for marine diesel engines. J Mech Eng Res Dev. 2018;41(4):22–3.

[7] Wu G, Jiang G, Chen C, Jiang G, Pu X, Chen B. An experimental study of the effects of cylinder lubricating oils on the vibration characteristics of a two-stroke low-speed marine diesel engine. Pol Marit Res. 2023;30(4):92–101.

[8] Marey Nour A, Wael M. Experimental study on hydro-thermal behavior of journal bearing oil film profile in a slow speed diesel engine. Alex Eng J. 2023;81:532–47.

[9] Tadros M, Ventura M. Optimization of the performance of marine diesel engines to minimize the formation of SOx emissions. J Mar Sci Appl. 2020;(19):473–84.

[10] Kukuljan D, Bernečić D, Orović J. The LNG reliquefaction plant – operating principle and justifiability of its installation on board ships. Pomorstvo. 2012;26(1):215–26.

[11] Aghdoudchaboki Y, Khoshgard A, Salehi GR, Fazelpour F. Thermoeconomic assessment of a waste heat recovery system driven by a marine diesel engine for power and freshwater production. Int J Exergy. 2020;33(3):231–53.

[12] Delprete C, Razavykia A. Piston dynamics, lubrication and tribological performance evaluation: a review. Int J Engine Res. 2020;21(5):725–41.

[13] Bernečić D, Šegulja I. Heat transfer influence analysis on combustion presure in two–stroke slow-speed marine diesel engines. Pomorstvo. 2013;27(1):73–85.

[14] Kutay Ş, Kamal B. Assessment of marine diesel engine crankshaft damages. Ships Offshore Struct. 2020;17(9):2130–9.

[15] Sinha RP, Balaji R. A mathematical model of marine diesel engine speed control system. J Inst Eng (India): Ser C. 2018;99(1):63–70.

[16] Zubkov EV, Novikov AA. Regulation of the crankshaft speed of a diesel engine with a common rail fuel system. Russian Eng Res. 2012;32(7–8):523–5.

[17] Li R, Meng X, Liu R, Muhammad R, Li W, Dong J. Crosshead bearing analysis for low-speed marine diesel engines based on a multi-body tribo-dynamic model. Int J Engine Res. 2021;22(8):2442–63.

[18] Choe S, Sun SX. Bending elasticity of anti-parallel β-sheets. Biophys J. 2007;92(4):1204–14.

[19] Ulenikov ON, Ditenberg EA, Olekhnovitch IM, Alanko S, Koivusaari M, Anttila R. Isotope substitution in near local mode molecules: bending overtonesnν_2 (n = 2, 3) of the HDS molecule. J Mol Spectrosc. 1998;191(2):239–47.

[20] Bisgrove SR. The roles of microtubules in tropisms. Plant Sci. 2008;175(6):747–55.

[21] Silva MJ, Brodt MD, Fan Z, Rho JY. Nanoindentation and whole-bone bending estimates of material properties in bones from the senescence accelerated mouse SAMP6. J Biomech. 2004;37(11):1639–46.

[22] Li T, Jiao B, Ma X, Lu X, Qiao Z. Optimization study of oil-feed parameters to improve the ring pack lubrication performance for a two-stroke marine diesel engine. Eng Fail Anal. 2022;137:106234.

[23] Lidui WEI, Hao C, Zhilei Z, et al. Mixed-lubrication analysis on main bearings of marine diesel engine taking crankshaft axial motion into account. Lubr Eng. 2023;48(6):0254–0150.

[24] Rossmanith HP. On cracked plates subjected to classical bending. Z für Angew Math Phys ZAMP. 1985;36(1):166–71.

[25] Meng X, Li R, Xie Y, Wang C. Simulation analysis and experimental verification of tribodynamics of reciprocating friction pairs in low-speed marine engines. Tribol Trans. 2023;66(3):576–96.

[26] Chen L, Xue D, Song X, He Z, Huang D. A study on anti-shock performance of marine diesel engine based on multi-body dynamics and elastohydrodynamic lubrication. Appl Sci. 2021;11(23):1–25.

[27] Nixon ME, Lebensohn RA, Cazacu O, et al. Experimental and finite-element analysis of the anisotropic response of high-purity α-titanium in bending. Acta Mater. 2010;58(17):5759–67.